Macromolecules
ARTICLE

Macromolecules **2010**, *43*, 6321–6329 **6321**
DOI: 10.1021/ma101136v

Synthesis of Biomimetic Poly(2-(methacryloyloxy)ethyl phosphorylcholine) Nanolatexes via Atom Transfer Radical Dispersion Polymerization in Alcohol/Water Mixtures

Shinji Sugihara,*,†,‡ Kana Sugihara (nee Nishikawa),‡ Steven P. Armes,*,‡ Hasan Ahmad,§ and Andrew L. Lewis⊥

†*Department of Applied Chemistry and Biotechnology, Graduate School of Engineering, University of Fukui, 3-9-1 Bunkyo, Fukui 910-8507, Japan,* ‡*Department of Chemistry, University of Sheffield, Brook Hill, Sheffield, South Yorkshire S3 7HF, U.K.,* §*Department of Chemistry, Rajshahi University, Rajshahi-6205, Bangladesh, and* ⊥*Biocompatibles UK Ltd., Chapman House, Farnham Business Park, Weydon Lane, Farnham, Surrey GU9 8QL, U.K.*

Received May 21, 2010; Revised Manuscript Received June 18, 2010

ABSTRACT: Poly(2-(methacryloyloxy)ethyl phosphorylcholine) (PMPC) exhibits a phenomenon known as co-nonsolvency in certain alcohol/water binary mixtures. We have exploited this phenomenon to prepare a series of sterically stabilized PMPC nanolatexes by atom transfer radical polymerization (ATRP) under dispersion polymerization conditions using a near-monodisperse poly(ethylene oxide) (PEO) macroinitiator in a 9:1 isopropanol/water mixture. The as-synthesized nanolatex particles comprised nonsolvated PMPC cores and solvated PEO shells, as determined by ^{1}H NMR spectroscopy. In our preliminary experiments linear core-forming PMPC chains were targeted, but alternatively either ethylene glycol dimethacrylate or bisphenol A dimethacrylate can be used as comonomers (at up to 10 mol % based on MPC) in order to prepare cross-linked PMPC particles that acquire swollen microgel character when dialyzed against pure water. Low levels of cross-linker (e.g., 4 mol %) lead to bimodal microgel size distributions as judged by dynamic light scattering. However, higher levels of cross-linker (e.g., 10 mol %) lead to narrow unimodal microgel size distributions, since all the core-forming PMPC chains become cross-linked. The final nanolatex/microgel dimensions are dictated by the target block compositions and initial MPC concentration used in these ATRP syntheses. A PEO_{113}-*b*-$PMPC_{50}$ formulation synthesized at 30 wt % solids produced nanolatex/microgel particles that were 5−6 times larger than those observed for the same block composition prepared at 10 wt % solids. TEM and SEM studies confirm that these new sterically stabilized particles have uniform spherical morphologies. Cross-linked PEO-*b*-PMPC particles were analyzed by X-ray photoelectron spectroscopy after dialysis against water. The surface coverage of the PEO stabilizer chains was estimated to be 54−61%. Aqueous electrophoresis studies confirmed that the PEO-*b*-PMPC microgels exhibited almost zero net charge, and the addition of electrolyte had little effect on their dimensions and colloidal stability due to the anti-polyelectrolyte behavior expected for the zwitterionic PMPC chains.

Introduction

Polymer latex particles are widely used for coatings, microelectronics, information technology, histological studies, immunodiagnostics, and drug delivery.[1−10] A narrow size distribution is often a key parameter for such applications. Several routes have been utilized to prepare near-monodisperse latexes. For example, aqueous emulsion polymerization uses a water-immiscible monomer in combination with a water-soluble initiator and typically produces uniform latexes of 100−500 nm diameter.[11−13] A useful alternative to this widely used process is dispersion polymerization, which can be regarded as a special type of precipitation polymerization conducted in the presence of a suitable polymeric stabilizer.[14] In dispersion polymerization, the monomer, initiator, and polymeric stabilizer are all initially soluble in the polymerization medium while the targeted polymer is not soluble. As the polymerization progresses, the monomer is converted into insoluble polymer and phase separation occurs. The polymeric stabilizer adsorbs onto the nascent microscopic nuclei and prevents macroscopic precipitation by a steric stabilization mechanism. Polymerization takes place mainly within the monomer-swollen droplets and, at the end of the polymerization, latex particles are obtained as a stable colloidal dispersion.[15,16] This versatile process can be conducted in many solvents, including water, and typically produces micrometer-sized latex particles.[17,18] Recent progress in controlled/living radical polymerization, particularly nitroxide-mediated polymerization (NMP),[19] atom transfer radical polymerization (ATRP),[20,21] and reversible addition−fragmentation chain transfer (RAFT) polymerization,[22] has led to the design and synthesis of novel well-defined polymer latexes. Dispersion polymerization formulations have proven to be particularly useful in this context.[23−26]

Over the past decade our group has demonstrated that ATRP can be used to prepare a wide range of controlled-structure block copolymers based on a commercially important biomimetic monomer, 2-(methacryloyloxy)ethyl phosphorylcholine (MPC).[27−30] Such MPC-based copolymers exhibit excellent biocompatibility,[31,32] suggesting various potential biomedical applications.[33−36] The unique properties (resistance to protein adsorption and bacterial adhesion, superlubricious surface coatings, etc.) imparted by PMPC-based copolymers are due to their highly

*To whom correspondence should be addressed: e-mail sugihara@u-fukui.ac.jp, Tel (+81)-776-27-9719, Fax (+81)-776-27-8747 (S.S.); e-mail s.p.armes@sheffield.ac.uk, Tel (+44)-114-222-9342, Fax (+44)-114-222-9346 (S.P.A.).

Published on Web 07/12/2010

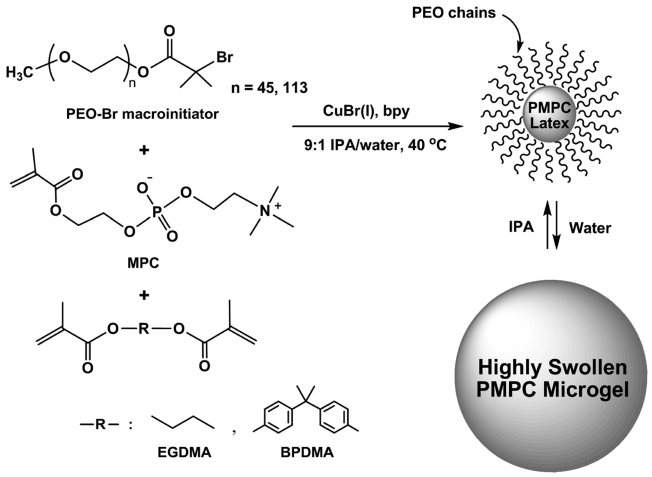

Figure 1. Synthesis of sterically stabilized cross-linked PEO-*b*-PMPC latex prepared via ATRP in a 9:1 IPA/water mixture at 40 °C.

hydrophilic character; it has been estimated that there are up to 22 water molecules per MPC repeat unit.[37,38] However, there have been only a few reports of MPC-based latex particles.[28,39−42]

PMPC homopolymer exhibits an unusual property known as co-nonsolvency in alcohol/water mixtures.[43] Although soluble in both lower alcohols and water, PMPC becomes insoluble in certain alcohol-rich alcohol/water mixtures.[29,30,43−45] Recently, we exploited this phenomenon for the synthesis of shell cross-linked micelles and nanocages. Thus, an ABC triblock copolymer, PEO-*b*-PDMA-*b*-PMPC [PDMA: poly(2-(dimethylamino)ethyl methacrylate)], was prepared in the form of PMPC-core micelles using ATRP in a 9:1 isopropanol (IPA)/water mixture that leads to co-nonsolvency.[29] Moreover, our group has also reported using conventional free radical chemistry for the dispersion polymerization of MPC in 9:1 IPA/water mixtures.[45] The resulting PMPC latexes were stabilized using a reactive poly(ethylene glycol) methacrylate (PEGMA) macromonomer. The mean latex diameter depended on both the PEGMA and initiator concentration, but only micrometer-sized latexes could be obtained using this formulation.

In the present study, we explore the ATRP synthesis of sterically stabilized PEO-*b*-PMPC *nanolatexes* via dispersion polymerization of MPC using a PEO-based ATRP macroinitiator in a 9:1 IPA/water mixture at 40 °C (see Figure 1). Since both PEO and PMPC are biocompatible, such nanolatexes are also expected to exhibit excellent biocompatibility, which should in turn confer stealthlike properties in vivo.[33,46] Ethylene glycol dimethacrylate (EGDMA) or bisphenol A dimethacrylate (BPDMA) was optionally used as a cross-linker to prevent dissolution of these particles when dialyzed against pure water. For optimized nanolatex formulations, this purification protocol leads to the formation of highly swollen microgels due to hydration of the PMPC cores. The effect of varying (i) the length of the core-forming PMPC chains and (ii) the MPC concentration on the final size of these new nanolatexes was examined using dynamic light scattering (DLS), scanning electron microscopy (SEM), and transmission electron microscopy (TEM). Aqueous electrophoresis and X-ray photoelectron survey spectroscopy (XPS) were utilized to characterize the surface composition of these particles, and ^{1}H NMR spectroscopy was used to assess the degree of PMPC core hydration in both alcohol/water mixtures and pure water.

Experimental Section

Materials. MPC was kindly donated by Biocompatibles UK Ltd. (Farnham, UK). EGDMA (98%) was purchased from Sigma-Aldrich UK, and its inhibitor was removed by column chromatography using activated basic alumina. Anhydrous isopropyl alcohol (IPA), copper(I) bromide [Cu(I)Br], 2,2′-bipyridine (bpy), BPDMA, and two monohydroxy-capped poly(ethylene oxides) with mean degrees of polymerization of 45 and 113 (designated PEO_{45}-OH, and PEO_{113}-OH, respectively) were purchased from Sigma-Aldrich UK and used as received. Fluorescein *O*-methacrylate (FMA; Sigma-Aldrich) was used as a fluorescent comonomer in selected latex syntheses without further purification. Both D_2O and d_8-IPA were purchased from Aldrich for ^{1}H NMR spectroscopy studies. Deionized water was used in all measurements. Silica gel 60 (0.063−0.200 μm, Merck) was used to remove the spent ATRP catalyst and was also used as received. PEO macroinitiators (PEO_{45}-Br and PEO_{113}-Br) were synthesized according to a well-known literature protocol.[47]

Synthesis of a Linear PEO-*b*-PMPC Nanolatex. The following representative example describes the synthesis of a linear PEO_{113}-*b*-$PMPC_{50}$ nanolatex. A similar protocol was used for all other non-cross-linked diblock copolymers. PEO_{113}-Br macroinitiator (0.631 g, 0.126 mmol, 1 equiv), bpy ligand (40 mg, 0.253 mmol, 2 equiv), and MPC (1.864 g, 6.31 mmol; DP = 50) were weighed into a round-bottomed flask and dissolved in a 9:1 w/w IPA/water mixture (22.458 g). After purging with nitrogen for 20 min, the Cu(I)Br catalyst (18 mg, 0.127 mmol, 1 equiv) was added quickly to the stirred solution under nitrogen. The total solids content of the reaction solution (i.e., the combined mass of the MPC monomer and the PEO_{113}-Br macroinitiator) was fixed at 10 wt %. The reaction mixture immediately became dark brown. The extent of the polymerization was monitored by ^{1}H NMR spectroscopy by analyzing aliquots taken from the reaction solution after quenching the polymerization by dilution with D_2O at 20 °C. After 24 h, ^{1}H NMR analysis indicated that more than 99% of the MPC had polymerized (disappearance of vinyl signals at 5.6 and 6.0 ppm). On exposure to air, the reaction solution turned blue, indicating aerial oxidation of the ATRP catalyst. The solution was diluted to 2.0 wt % using a 9:1 IPA/water mixture, followed by purification using silica chromatography to remove the spent ATRP catalyst.

Synthesis of a Cross-Linked PEO-*b*-PMPC Nanolatex. The following example describes the synthesis of a cross-linked PEO_{113}-*b*-$PMPC_{50}$ nanolatex using 10 mol % EGDMA comonomer based on MPC. This protocol is representative of all cross-linked nanolatex syntheses. PEO_{113}-Br macroinitiator (0.631 g, 0.126 mmol, 1 equiv), bpy ligand (40 mg, 0.253 mmol, 2 equiv), MPC (1.864 g, 6.31 mmol; DP = 50), and EGDMA cross-linker (0.125 g, 0.631 mmol) were weighed into a round-bottomed flask and dissolved in a 9:1 w/w IPA/water mixture (23.533 g). After purging with nitrogen for 20 min, the Cu(I)Br catalyst (18 mg, 0.127 mmol, 1 equiv) was added quickly to the stirred solution under nitrogen. The total solids content of the reaction solution (i.e., the combined mass of MPC, PEO_{113}-Br macroinitiator, and EGDMA cross-linker) was fixed at 10 wt %. After polymerization had been initiated, the reaction mixture immediately became dark brown. The extent of polymerization was again monitored by ^{1}H NMR spectroscopy. After 48 h, ^{1}H NMR analysis indicated that more than 99% of the MPC had polymerized (disappearance of vinyl signals at 5.6 and 6.0 ppm). On exposure to air, the reaction solution turned blue, indicating aerial oxidation of the ATRP catalyst. The solution was diluted to desired concentration using a 9:1 IPA/water mixture, followed by purification using silica chromatography to remove the spent ATRP catalyst. For the PEO-*b*-PMPC nanolatex containing fluorescent FMA comonomer (2 mol % based on MPC), PEO_{113}-Br macroinitiator (0.631 g, 0.126 mmol, 1 equiv), bpy ligand (40 mg, 0.253 mmol, 2 equiv), MPC (1.864 g, 6.31 mmol; DP = 50), FMA (0.050 g, 0.126 mmol), and EGDMA cross-linker (0.125 g, 0.631 mmol) were weighed into a round-bottomed flask and dissolved in a 9:1 IPA/water mixture

(24.030 g). After purging with nitrogen for 20 min, the Cu(I)Br catalyst (18 mg, 0.127 mmol, 1 equiv) was added quickly to the stirred solution under nitrogen, and the polymerization was initiated. In the case of the BPDMA cross-linker, PEO_{113}-Br macroinitiator (0.631 g, 0.126 mmol, 1 equiv), bpy ligand (40 mg, 0.253 mmol, 2 equiv), MPC (1.864 g, 6.31 mmol; DP = 50), and BPDMA cross-linker (0.230 g, 0.631 mmol) were weighed into a round-bottomed flask and dissolved in a 9:1 IPA/water mixture (24.492 g). After purging with nitrogen for 20 min, the Cu(I)Br catalyst (18 mg, 0.127 mmol, 1 equiv) was added quickly to the stirred solution under nitrogen. To prepare PEO-*b*-PMPC particles in their swollen microgel form, the corresponding PEO-*b*-PMPC latex in a 9:1 IPA/water was dialyzed against pure water for 3 days using Spectra/Por cellulose tubing (molecular weight cutoff = 1000). This protocol removed almost all of the toxic ATRP catalyst, since the initially blue nanolatex particles became white after purification. On the basis of our previous experience, this suggests that any residual copper does not exceed the ppm level.[47]

Characterization of PEO-*b*-PMPC Block Copolymers and Nanolatexes. *Size Exclusion Chromatography* (*SEC*). Molecular weight distributions were assessed by SEC using a Hewlett-Packard HP1090 liquid chromatograph pumping unit and two Polymer Laboratories PL Gel 5 μm Mixed-C (7.5 × 300 mm) columns in series with a guard column at 40 °C connected to a Gilson model 131 refractive index detector. The eluent was a 3:1 v/v chloroform/methanol mixture containing 2 mM LiBr at a flow rate of 1.0 mL/min. The number-average molecular weight (M_n) and polydispersity (M_w/M_n) were calculated from SEC curves using near-monodisperse poly(methyl methacrylate) (PMMA) calibration standards.

^{1}H NMR Spectroscopy. All ^{1}H NMR spectra were recorded in either D_2O or 9:1 d_8-IPA/D_2O mixture using a Bruker AV1-400 MHz spectrometer.

Dynamic Light Scattering (*DLS*) *and Aqueous Electrophoresis*. DLS studies were performed using a ZetaSizer Nano-ZS instrument (Malvern Instruments, UK) at 25 °C at a scattering angle of 173° using 0.20 wt % dispersions of the PEO-*b*-PMPC nanolatexes in either pure water or a 9:1 IPA/water mixture. The intensity-average hydrodynamic diameter (D_h) and polydispersity (PDI, μ_2/Γ^2) were calculated by cumulants analysis of the experimental correlation function using Dispersion Technology software version 5.03. The deionized water used to dilute each block copolymer or latex was ultrafiltered through a 0.2 μm membrane so as to remove extraneous dust. A literature value of 2.3259 cP was used for the solution viscosity of the 9:1 IPA/water mixture.[49] For cross-linked PEO-*b*-PMPC nanolatexes dispersed as aqueous swollen microgels in the presence of varying amounts of NaCl, the appropriate solution viscosities were calculated using data provided in the manufacturer's software. Aqueous electrophoresis studies were also conducted for selected PEO-*b*-PMPC microgels dispersed in water using the same ZetaSizer Nano-ZS instrument. Zeta potentials were calculated from mobilities using the Henry equation and determined as a function of solution pH at 25 °C. Dilute aqueous solutions of HCl and NaOH were used for pH adjustment.

X-ray Photoelectron Spectroscopy (*XPS*). The surface composition of cross-linked PEO_{113}-*b*-$PMPC_{50}$ particles was evaluated using a Kratos Axis Ultra DLD X-ray photoelectron spectrometer equipped with a monochromatic Al X-ray source operating at 6.0 mA and 15 kV with a typical base pressure of 10^{-8} Torr. The step size was 1.0 eV for the survey spectra (pass energy 160 eV) and 0.1 eV for the high-resolution spectra (pass energy 80 eV). In each case, the particles were dried from pure water (i.e., in their swollen microgel form) onto a planar silicon wafer prior to analysis.

Scanning Electron Microscopy (*SEM*). A few drops of a dilute nanolatex dispersed in a 9:1 IPA/water mixture were placed on an adhesive carbon disk and then were dried at room temperature. Samples were then sputter-coated with an ultrathin layer of gold prior to observation using an FEI Inspect F FEG instrument operating at 20 kV and a beam current of 244 μm.

Transmission Electron Microscopy (*TEM*). TEM studies were conducted using a Philips CM 100 instrument operating at 100 kV equipped with a Gatan 1 k CCD camera. Carbon-coated copper grids were subjected to a glow discharge for 20−30 s to create a hydrophilic surface. Grids were then immersed in selected PEO-*b*-PMPC nanolatex/microgel dispersions for 1 min and then immersed for 20 s in a uranyl acetate solution (0.75% w/v) for negative staining. Each grid was then blotted with filter paper and dried using a vacuum hose.

Results and Discussion

Initially, we examined the ATRP of MPC in the absence of any cross-linker using a PEO_{113}-Br macroinitiator and CuBr/bpy catalyst in a 9:1 IPA/water mixture at 40 °C targeting a DP of 50. The MPC monomer is fully soluble in this mixed solvent from 20 to 40 °C. However, PMPC is insoluble in this particular solvent mixture due to its well-known co-nonsolvency behavior.[29,30,43−45] Thus, these ATRP syntheses proceed under dispersion polymerization conditions to produce linear PEO-*b*-PMPC nanolatexes.

Using $[MPC]_0/[PEO_{113}\text{-Br}]_0/[CuBr]_0/[bpy]_0$ relative molar ratios of 50:1:1:2, the ATRP of MPC reached almost complete conversion within around 5 h at 40 °C at 10 wt % solids in a 9:1 IPA/water mixture. Initially, the solution was homogeneous, but as the polymerization progressed, the reaction mixture became opaque, with the dark-brown coloration originating from the ATRP catalyst being maintained. Monomer conversions were calculated from diluted aliquots of the reaction solution using ^{1}H NMR spectroscopy in D_2O by comparing the integrated monomer vinyl resonances at 5.6−6.0 ppm to the signal due to three quaternary nitrogen methyl groups at 3.1−3.2 ppm. These kinetic studies afforded a linear semilogarithmic plot (see Figure 2a), indicating first-order kinetics with respect to monomer. SEC analyses of aliquots taken from the MPC polymerization using a 3:1 $CHCl_3/CH_3OH$ eluent containing 2 mM LiCl indicated a linear increase in molecular weight with conversion (see Figure 2b). Moreover, polydispersities remained relatively narrow throughout the polymerization (but increased slightly toward the end of the polymerization, e.g., M_w/M_n = 1.18 at 47% conversion and M_w/M_n = 1.22 at 99% conversion).

Figure 3 shows typical SEC chromatograms obtained for linear PEO-*b*-PMPC block copolymers grown from a PEO_n-Br macroinitiator (where n = 45 or 113) under dispersion polymerization conditions. The PEO-*b*-PMPC block composition was determined by ^{1}H NMR spectroscopy (see Figure 4c). The integrated intensity of the nine trimethylammonium protons due to the MPC residues at 3.1−3.2 ppm (peak a in Figure 4c) was compared to a complex peak at 3.5−3.6 ppm due to both the ethylene oxide protons of the PEO chains and also the azamethylene protons of the MPC residues (peaks b and i in Figure 4c). Table 1 summarizes the target and actual block compositions, number-average molecular weights (M_n), and polydispersities (M_w/M_n) for the various linear PEO-*b*-PMPC diblock copolymers prepared in this study, as calculated from the SEC and ^{1}H NMR data. Block copolymer molecular weight distributions are shifted to significantly higher molecular weights relative to the PEO_n-Br macroinitiator, regardless of the macroinitiator chain length (n) and target block composition. However, in the case of PEO_{45}-Br (see entry 1 in Table 1 and Figure 3a), there is a prominent shoulder corresponding to unreacted PEO_{45}-Br macroinitiator. Thus, the macroinitiator efficiency is not perfect based on the SEC chromatograms. However, the PEO_{113}-Br macroinitiator seems to be somewhat better than the PEO_{45}-Br macroinitiator. Thus, we mainly used PEO_{113}-Br macroinitiator to prepare the PEO−PMPC latexes. Moreover, the actual block

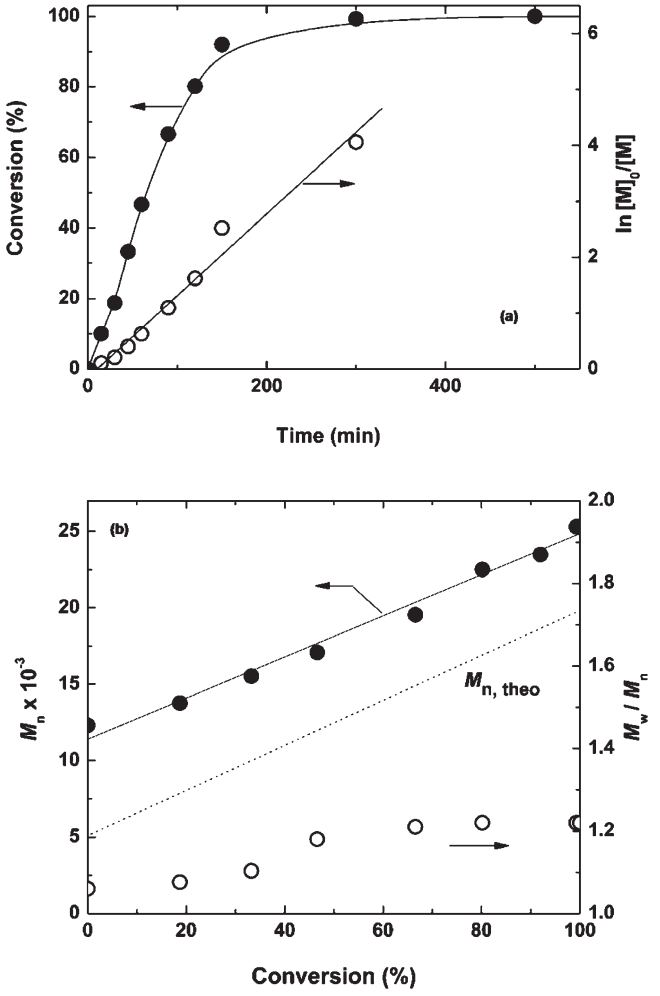

Figure 2. (a) Kinetic plots and (b) M_n (●), theoretical M_n (···) and polydispersity (○) as a function of monomer conversion for ATRP in 9:1 IPA/water at 40 °C: MPC (6.31 mmol), PEO_{113}-Br (0.126 mmol), $[PEO_{113}\text{-Br}]_0/[Cu(I)Br]_0/[bpy]_0$ = 1:1:2; solid content = 10 wt %. The obtained M_n was calculated using PMMA standards.

compositions for block copolymers prepared from PEO_{113}-Br were in reasonably good agreement with the targeted compositions, suggesting that reasonably good living character was achieved under these conditions.

Table 1 also summarizes the hydrodynamic diameter (D_h) of each PEO-*b*-PMPC linear latex dispersed in a 9:1 IPA/water mixture as determined by DLS. For a series of PEO_{113}-*b*-$PMPC_m$ block copolymers, as the DP of the PMPC block was increased from 25 to 75, the mean diameter increased from 53 to 99 nm (compare entries 2−4). It is well-documented that larger micelles are invariably obtained when the chain length of the core-forming block is increased.[50] These DLS results confirm that the polymerization of MPC from PEO-Br macroinitiator drives in situ block copolymer self-assembly in a 9:1 IPA/water mixture to produce sterically stabilized nanolatexes. The D_h of a PEO_{45}-*b*-$PMPC_{50}$ latex (see entry 1) is bigger than that of a PEO_{113}-*b*-$PMPC_{50}$ latex, suggesting that shorter PEG blocks favor the formation of larger nanolatexes as expected.

To confirm micellar self-assembly, the ^{1}H NMR spectrum of a PEO_{113}-*b*-$PMPC_{50}$ diblock copolymer (see entry 3) was recorded both in a 9:1 d_8-IPA/D_2O mixture and also in pure D_2O. In the latter solvent, all the signals expected for both blocks were well-resolved, suggesting true molecular dissolution under these conditions (see Figure 4c). Signals a and b are characteristic of the

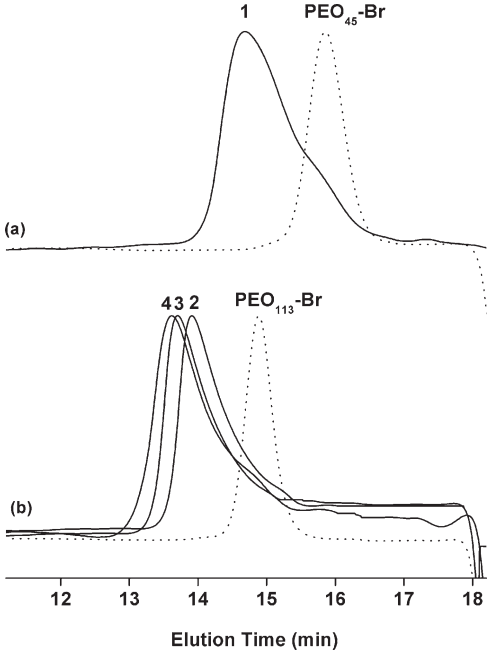

Figure 3. Typical SEC curves for PEO_n-*b*-$PMPC_m$ block copolymers obtained from PEO_n-Br macroinitiator: (a) n = 45 and (b) n = 113. The target degree of PMPC block for **1**, **2**, **3**, and **4** is 50, 25, 50, and 75, respectively (see entries 1−4 in Table 1): MPC (3.16−9.47 mmol), PEO_n-Br (n = 45 or 113, 0.126 mmol), $[PEO_n\text{-Br}]_0/[Cu(I)Br]_0/[bpy]_0$ = 1:1:2 dissolved in a 9:1 IPA/water mixture; solid content = 10 wt %, polymerization time = 24 h (PEO_{45}-Br: M_n 4700, M_w/M_n 1.08; PEO_{113}-Br: M_n 12 300, M_w/M_n 1.06, calculated by PMMA standards).

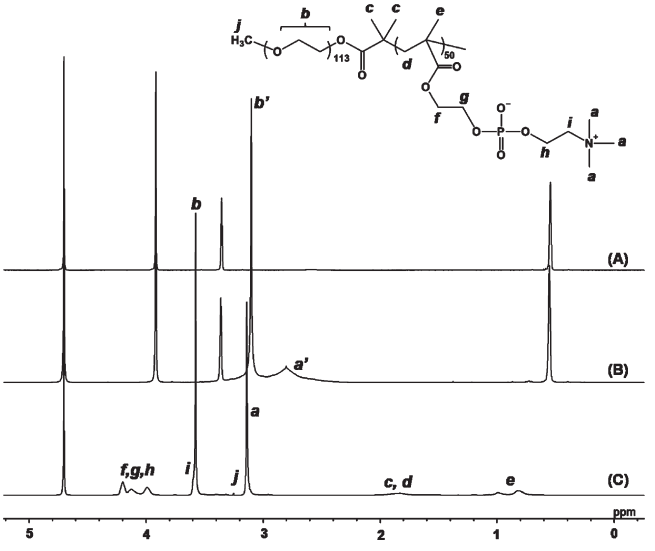

Figure 4. Typical ^{1}H NMR spectra recorded for PEO_{113}-*b*-$PMPC_{50}$ block copolymer (entry 3 in Table 1) in various solvents: (A) 9:1 d_8-IPA/D_2O mixture only (no copolymer); (B) 9:1 d_8-IPA/D_2O mixture; (C) D_2O. Signals a and b are characteristic of the PEO and PMPC blocks, respectively. These are shifted by adding d_8-IPA: a → a′ and b → b′.

PMPC and PEO blocks, respectively. In a 9:1 d_8-IPA/D_2O mixture (see Figure 4b), all the copolymer signals were shifted upfield relative to HDO at 4.7 ppm. Furthermore, all the signals assigned to the PMPC chains broadened significantly (a → a′), whereas the main peak due to the PEO block remained relatively sharp (b → b′). These observations are consistent with the formation of PMPC-core micelles at this particular solvent composition.

Our initial syntheses of linear PEO-*b*-PMPC latex particles were extended to include cross-linked PEO-*b*-PMPC nanolatexes

Table 1. ATRP Synthesis of Linear PEO-*b*-PMPC Diblock Copolymers at 40 °C in 9:1 IPA/Water Mixtures[a]

entry	target block composition[b]	actual block composition[c]	M_n[d]	M_w/M_n[d]	D_h/nm (PDI) in 9:1 IPA/water[e]
1	PEO_{45}-*b*-$PMPC_{50}$	PEO_{45}-*b*-$PMPC_{53}$	13 800	1.26	143 (0.201)
2	PEO_{113}-*b*-$PMPC_{25}$	PEO_{113}-*b*-$PMPC_{27}$	20 400	1.22	53 (0.082)
3	PEO_{113}-*b*-$PMPC_{50}$	PEO_{113}-*b*-$PMPC_{50}$	25 300	1.22	72 (0.082)
4	PEO_{113}-*b*-$PMPC_{75}$	PEO_{113}-*b*-$PMPC_{75}$	32 700	1.23	99 (0.109)

[a] Polymerization conditions (see also Figure 3). [b] Calculated from the feed molar ratio of MPC and PEO-Br macroinitiator. [c] Determined by ^{1}H NMR: conversion >99%, assuming that the blocking efficiency is 100%. [d] Determined by SEC (PMMA standards, 3:1 chloroform/methanol mixed eluent containing 2 mM LiCl). [e] At 25 °C.

Table 2. Various PEO_{113}-*b*-$PMPC_m$ Nanolatexes Synthesized by ATRP in 9:1 IPA/Water Mixtures at 40 °C Using Either EGDMA or BPDMA Cross-Linker[a]

entry	target DP of MPC[b]	actual DP of MPC[c]	cross-linker[d]	$[\text{cross-linker}]_0/[\text{MPC}]_0$ (mol %)	solid (wt %)[e]	D_h/nm (PDI) in 9:1 IPA/water[f,g]	D_h/nm (PDI) in water[g]
5	50	51	E	4.0	10.0	104 (0.079)	
6	50	50	E	8.0	10.0	90 (0.082)	
7	50	50	E	10.0	10.0	82 (0.082)	171 (0.156)
8[h]	50	49	E	10.0	10.0	97 (0.051)	148 (0.289)
9	50	51	E	12.0	10.0	76 (0.059)	144 (0.136)
10	50	53	E	10.0	15.0	50 (0.128)	81 (0.153)
11	50	50	E	10.0	20.0	78 (0.154)	114 (0.097)
12	50	51	E	10.0	25.0	294 (0.100)	426 (0.199)
13	50	51	E	10.0	30.0	512 (0.103)	830 (0.143)
14	25	26	E	20.0	10.0	63 (0.120)	107 (0.086)
15	75	77	E	6.7	10.0	95 (0.017)	180 (0.233)
16	100	105	E	5.0	10.0	188 (0.012)	
17	50	50	B	10.0	10.0	68 (0.097)	207 (0.215)
18[i]	50	49	E	10.0	10.0	174 (0.054)	297 (0.112)

[a] PEO_{113}-Br (0.126 mmol), $[PEO_{113}\text{-Br}]_0/[Cu(I)Br]_0/[bpy]_0 = 1:1:2$, polymerization time = 48 h. [b] Calculated from $[MPC]_0/[PEO_{113}\text{-Br}]_0$. [c] Determined by ^{1}H NMR: conversion >99%. [d] E: EGDMA, B: BPDMA. [e] 100 × [PEO_{113}-Br (g) + MPC (g) + cross-linker (g)]/[all reaction mixtures excluding Cu(I)Br and bpy (g)]. [f] Solution viscosity of a 9:1 IPA/water mixture was taken to be 2.3259 cP at 25 °C. [g] At 25 °C. [h] Including in FMA units in the latex: MPC (6.31 mmol), EGDMA (0.631 mmol), PEO_{113}-Br (0.126 mmol), FMA (0.126 mmol), $[PEO_{113}\text{-Br}]_0/[Cu(I)Br]_0/[bpy]_0 = 1:1:2$, polymerization time = 48 h. [i] PEO_{45}-Br was used as a macroinitiator instead of PEO_{113}-Br.

using either EDGMA or BPDMA comonomers (ranging from 4 to 12 mol % cross-linker). This is important, since the linear nanolatexes do not survive in their colloidal form in pure water because the core-forming PMPC chains become hydrated under these conditions. Thus, cross-linking prevents nanolatex dissolution, which is essential if these particles are to be used for biomedical applications. Table 2 summarizes all the cross-linked PEO-*b*-PMPC latex syntheses. In all cases, similar results were obtained to the linear nanolatex formulations containing no cross-linker. The solution gradually became opaque as the polymerization progressed, and colloidally stable latexes were obtained in a 9:1 IPA/water mixture with no trace of any precipitation. As-synthesized latexes were diluted using the same 9:1 IPA/water mixture, followed by purification using silica chromatography to remove the spent ATRP catalyst. The final conversions and block compositions were determined by ^{1}H NMR spectroscopy, and the latter were in good agreement with the target compositions. However, the colloidal stability of these nanolatexes after prolonged dialysis against water depended on their cross-linker content. Entries 5−9 in Table 2 show the effect of EGDMA content for PEO_{113}-*b*-$PMPC_{50}$ nanolatexes prepared at 10 wt % solids, while Figure 5 shows the typical intensity-average particle size distributions obtained for selected cross-linked PEO_{113}-*b*-$PMPC_{50}$ nanolatexes in both 9:1 IPA/water and in pure water. Nanolatexes with mean D_h values of 76−104 nm were obtained in 9:1 IPA/water mixtures, regardless of EGDMA content. Typically, each D_h is slightly bigger than that obtained in a 9:1 IPA/water mixture formed by the corresponding linear PEO-*b*-PMPC nanolatexes. As the EGDMA content was increased from 4 to 12 mol % (based on MPC), the D_h decreased from 104 to 76 nm, and the corresponding polydispersity was reduced from 0.079 to 0.059, respectively. More importantly, a bimodal size distribution was observed for a cross-linked PEO_{113}-*b*-$PMPC_{50}$ nanolatex prepared using 4 mol % EGDMA cross-linker after dialysis against water (Figure 5a).

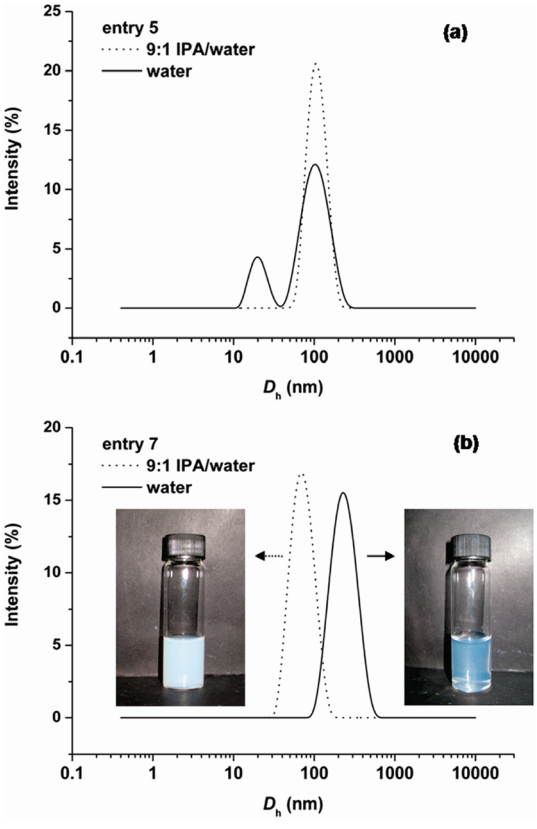

Figure 5. Typical intensity-average particle size distributions for EGDMA cross-linked PEO_{113}-*b*-$PMPC_{50}$ latexes in a 9:1 IPA/water mixture (···) and in water after dialysis (—): see (a) entry 5 and (b) entry 7 in Table 2. Only the latter sample is fully cross-linked.

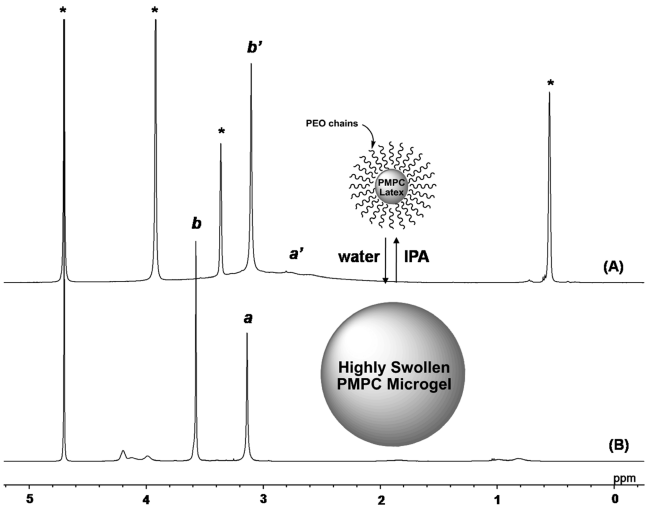

Figure 6. Typical ^{1}H NMR spectra recorded for an EGDMA-cross-linked PEO_{113}-*b*-$PMPC_{50}$ nanolatex (entry 7 in Table 2) in (A) 9:1 d_8-IPA/D_2O and (B) pure D_2O. Signals a and b are characteristic of the PEO and PMPC blocks, respectively. These signals are shifted on swelling: a′ → a and b′ → b. The asterisks denote solvent peaks.

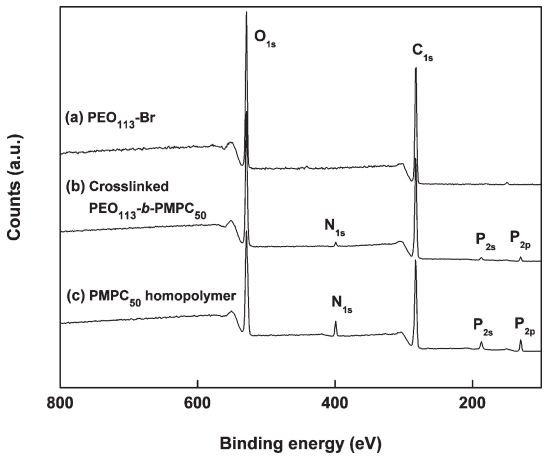

Figure 7. X-ray photoelectron survey spectra recorded for (b) EGDMA cross-linked PEO_{113}-*b*-$PMPC_{50}$ particles (entry 7 in Table 2) dried from their swollen microgel form in water, (a) PEO_{113}-Br macroinitiator, and (c) PMPC homopolymer.

The major population corresponds to swollen microgel particles of ~100 nm diameter, while the smaller secondary population at 10−30 nm corresponds to a soluble fraction of non-cross-linked copolymer chains. However, on increasing the EGDMA content to 10 mol %, only a single population of near-monodisperse, highly swollen PEO_{113}-*b*-$PMPC_{50}$ microgels was obtained (see Figure 5b). If cross-linking had been unsuccessful, no swollen microgels would exist after dialysis against water since molecular dissolution should occur. On increasing the EGDMA content further from 10 to 12 mol %, the D_h is reduced from 171 to 144 nm and the polydispersity decreased from 0.156 to 0.136, respectively, indicating higher degrees of cross-linking and hence reduced swelling of the PMPC cores. PEO_{113}-*b*-$PMPC_{50}$ latexes were also obtained using 10 mol % BPDMA cross-linker rather than EGDMA (see entry 17 in Table 2). Comparing entries 7 and 15 in Table 2, the cross-linked PEO_{113}-*b*-$PMPC_{50}$ latex prepared using BPDMA is somewhat smaller in the 9:1 IPA/water mixture but becomes more swollen in pure water. This indicates less efficient cross-linking with this alternative cross-linker. This suggests that the relatively hydrophobic BPDMA cross-linker may be less well solubilized within the ionic PMPC cores (and hence partially excluded from them) during the dispersion polymerization of MPC. It is also worth emphasizing that similarly inefficient cross-linking was achieved using a disulfide-based dimethacrylate cross-linker[51] even at a target degree of cross-linking of 20 mol %.

To prepare fluorescent cross-linked PEO_{113}-*b*-$PMPC_{50}$ latex, FMA was introduced into the nanolatex formulation as a minor comonomer (see entry 8 in Table 2). This copolymerization also proceeded smoothly, and the final nanolatex had a yellowish color. Additional aromatic signals were visible at 6.5−8.5 ppm as confirmed by ^{1}H NMR spectroscopy (data not shown), and the dimensions of this nanolatex/microgel were comparable to entry 7. Unfortunately, this fluorescently labeled latex was too small to be observed by confocal laser scanning microscopy. However, it may prove to be an interesting model stealthy nanoparticle for phagocytosis studies.[45]

Figure 6 shows the ^{1}H NMR spectra recorded for a cross-linked PEO_{113}-*b*-$PMPC_{50}$ nanolatex/microgel prepared using 10 mol % EGDMA (see entry 7 in Table 2) in both a 9:1 d_8-IPA/D_2O mixture and also pure D_2O. In the latter case (see Figure 6b), all the characteristic peaks expected for the PMPC and PEO chains are visible despite cross-linking of the PMPC chains, suggesting that highly swollen microgels are formed under these conditions. As expected, all these copolymer signals were shifted upfield relative to HDO at 4.7 ppm. All the PMPC signals either broadened (see a′) or disappeared in a 9:1 d_8-IPA/D_2O mixture, whereas the PEO signal remained relatively sharp (see Figure 6a). This indicates that the coronal PEO chains remain well-solvated under both conditions, whereas the PMPC core is desolvated in a 9:1 d_8-IPA/D_2O mixture but becomes highly hydrated in D_2O. This PEO_{113}-*b*-$PMPC_{50}$ nanolatex exhibited excellent colloidal stability on storage at 20 °C for more than 6 months, with no significant variation in the mean particle diameter being observed.

XPS was used to examine the surface composition of PEO_{113}-*b*-$PMPC_{50}$ particles after drying from its swollen microgel state. Figure 7 shows the survey spectra recorded for cross-linked PEO_{113}-*b*-$PMPC_{50}$ particles (entry 7 in Table 2), with a PEO_{113}-Br macroinitiator and a PMPC homopolymer included as reference materials. Comparing the C_{1s}, N_{1s}, O_{1s}, P_{2s}, and P_{2p} core-line spectra, it is clear that the PEO and PMPC chains are both present in the near-surface of the PEO−PMPC particles (the typical XPS analysis depth is ~2−8 nm). Unfortunately, the O_{1s} and C_{1s} spectra of PEO_{113}-*b*-$PMPC_{50}$ particles do not differ significantly from the corresponding spectra obtained for PEO_{113}-Br and PMPC homopolymer. However, the P_{2p} signal intensity of 130 eV corresponds to ~2.3 atom % for the cross-linked PEO_{113}-*b*-$PMPC_{50}$ latex and ~5.0 atom % for PMPC homopolymer. Similarly, the N_{1s} signal intensity at 399 eV for the cross-linked PEO_{113}-*b*-$PMPC_{50}$ particles was ~1.2 atom % but ~3.1 atom % for the PMPC homopolymer. In both cases, this signal attenuation is attributed to the presence of the PEO steric stabilizer chains at the surface of the PMPC particles. From these results, the PEO surface coverage is estimated to be 54−61%.

Figure 8 shows the effect of increasing the MPC and PEO macroinitiator concentrations on the final nanolatex dimensions. Comparing the 10 and 15 wt % formulations, the latter yielded a smaller nanolatex (82 nm vs 50 nm diameter; see entries 7 and 10 in Table 2). The volumetric swelling factors determined by DLS for the two corresponding swollen microgels obtained after dialysis confirmed that the smaller nanolatex had a significantly higher degree of cross-linking. This is consistent with our recent findings with soluble branched copolymers, where higher monomer concentrations favor intermolecular branching (or cross-linking) over intramolecular cyclization.[51] This interpretation is corroborated by the observation that increasing the proportion

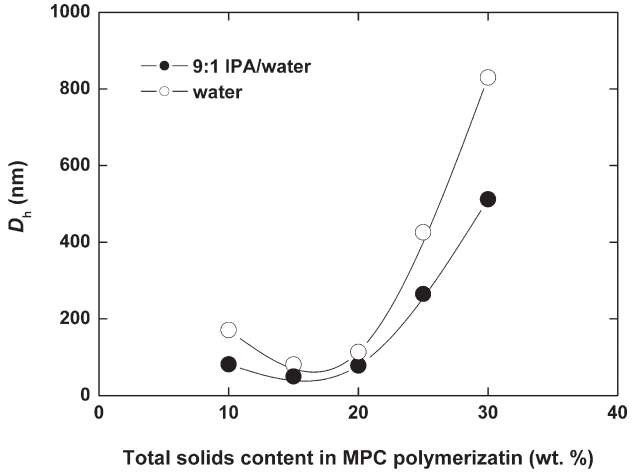

Figure 8. Effect of varying the total solids content used in the MPC polymerization on the final particle diameter, as determined in a 9:1 IPA/water mixture (●) and in water (after prolonged dialysis against water) (○) at 25 °C. These samples correspond to entries 7 and 10−13 in Table 2.

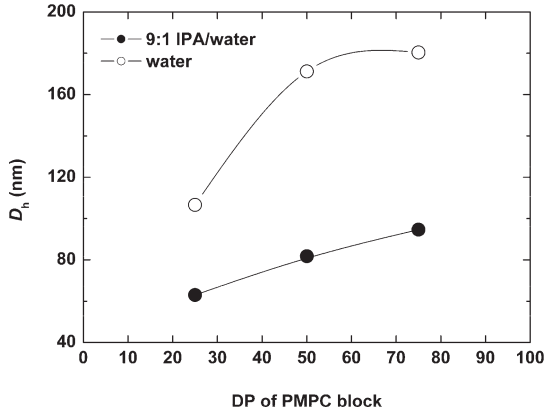

Figure 9. Effect of varying the target degree of polymerization of the PMPC block on the particle diameter at 25 °C in a 9:1 IPA/water mixture (●) and in water (after prolonged dialysis against water) (○). These samples correspond to entries 7, 14, and 15 in Table 2.

of EGDMA comonomer used in a 10% formulation also led to a reduction in mean particle diameter from 82 to 76 nm (compare entries 7 and 9 in Table 2). However, on further increasing the solids content for the MPC polymerization from 15 up to 30 wt %, significantly larger cross-linked latexes and microgels were obtained (512 nm diameter in a 9:1 IPA/water mixture and 830 nm diameter in pure water; entry 13 in Table 2). This concentration-dependent particle size effect is typically observed for (non)aqueous dispersion polymerizations.[52,53] DLS studies indicated that narrow, unimodal size distributions are typically obtained both before and after dialysis. This suggests that cross-linking is relatively efficient under these conditions since there is no evidence for any soluble fraction of PMPC chains. SEM and TEM studies confirmed a spherical morphology for the latex obtained from the 30 wt % formulation (see Figure 10). Overall, our results confirm that the mean nanolatex diameter can be controlled over a wide range (from 50 to 512 nm) simply by appropriate adjustment of the synthesis parameters.

The effect of varying the PMPC block length on the final latex diameter was also examined (see Figure 9; entries 7 and 14−16 in Table 2). In this series of experiments, the total solids content for each polymerization was fixed at 10 wt %. As the target degree of polymerization of the PMPC block was varied from 25 to 100, the mean nanolatex diameter determined in the 9:1 IPA/water

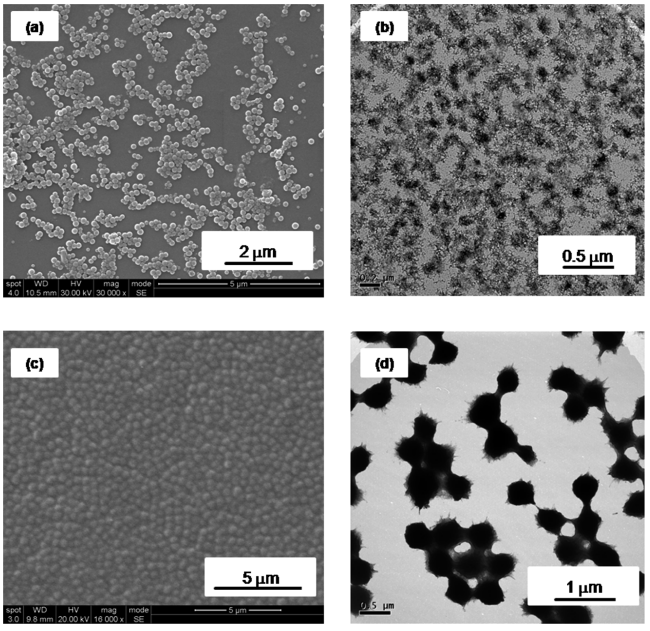

Figure 10. SEM (a, c) and TEM (b, d) images of selected PEO-*b*-PMPC latexes and microgels. SEM samples were prepared by air-drying from 9:1 IPA/water mixtures. For TEM images, PEO-*b*-PMPC latexes were dialyzed against water and stained with uranyl acetate: (a) entry 8 in 9:1 IPA/water; (b) entry 7 in water; (c) entry 13 in 9:1 IPA/water; (d) entry 13 in water.

mixture increased from 63 to 188 nm as judged by DLS. Moreover, in each case relatively low polydispersities were obtained. Similar results were observed for the linear PEO-*b*-PMPC nanolatexes (see above). However, DLS studies of the cross-linked PEO_{113}-*b*-$PMPC_{100}$ particles (see entry 16 in Table 2) indicated a trimodal size distribution, which suggests a soluble fraction. ^{1}H NMR confirmed that the MPC polymerization proceeded to more than 99% conversion, so it is not clear why cross-linking should be relatively inefficient in this case. In principle, it should be easier to cross-link longer PMPC chains using EGDMA than shorter chains. Further work will be required in order to rationalize this puzzling result. With the exception of this anomalous entry, the mean diameter of the swollen microgels obtained after dialysis increased as the target degree of polymerization of the PMPC block was systematically varied from 25 to 75, as expected.

Figure 10 shows typical SEM and TEM images obtained for cross-linked PEO_{113}-*b*-$PMPC_{50}$ particles synthesized at 10 wt % solids (see entry 8) and dried from their nanolatex and swollen microgel states, respectively. In Figure 10a, spherical, reasonably monodisperse nanolatex particles with a number-average diameter of ∼160 nm are observed. This image was obtained after allowing the particles dispersed in a 9:1 IPA/water mixture to dry on the grid in room temperature. The latex diameter was slightly larger than the corresponding DLS diameter (see Table 2). This suggests that either particle swelling or latex spreading occurred during sample preparation. The heights of these dried nanolatexes were around 20−25 nm, as judged by tapping-mode AFM topological images acquired using a Nanoscope IIIa scanning probe microscope (Veeco Instruments; data not shown). A cross-linked PEO_{113}-*b*-$PMPC_{50}$ latex had a microgel diameter of ∼140 nm after dialysis against water, although this image is only poorly resolved (see Figure 10b). Representative SEM and TEM images recorded for cross-linked PEO_{113}-*b*-$PMPC_{50}$ particles synthesized at 30 wt % solids are shown in Figure 10c and 10d. The observed number-average diameter of around 500 nm is consistent with DLS data obtained for this latex.

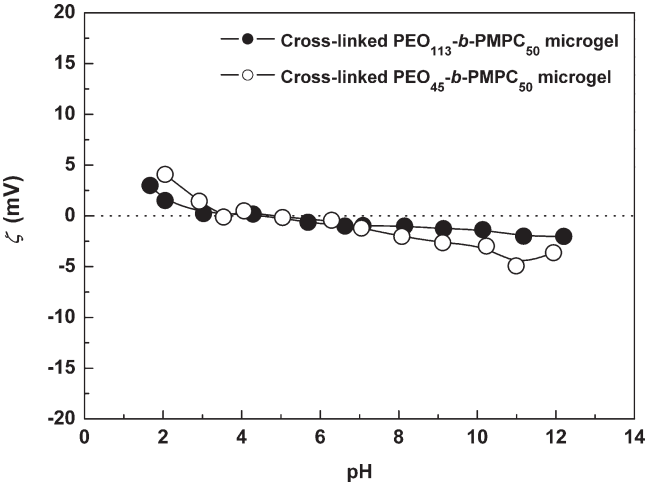

Figure 11. Zeta potential vs pH curves obtained for dilute aqueous dispersions of EGDMA cross-linked PEO_{113}-*b*-$PMPC_{50}$ microgel (●, entry 7) and PEO_{45}-*b*-$PMPC_{50}$ microgel (○, entry 18). These swollen microgels were obtained after prolonged dialysis against water.

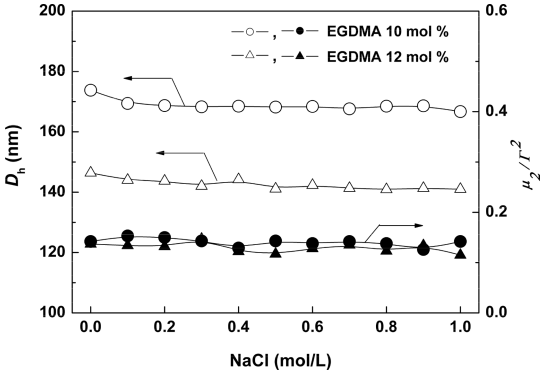

Figure 12. Effect of addition of NaCl on the intensity-average diameter and polydispersity at 25 °C for EGDMA cross-linked PEO_{113}-*b*-$PMPC_{50}$ microgels (entries 7 and 9; for which EGDMA = 10 or 12 mol %, respectively) dispersed in water.

Figure 11 shows aqueous electrophoresis curves obtained for cross-linked PEO_{113}-*b*-$PMPC_{50}$ and PEO_{45}-*b*-$PMPC_{50}$ nanolatexes (entries 7 and 18, respectively) as a function of pH. These particles formed well-defined, near-monodisperse swollen cross-linked microgels after dialysis against water. Regardless of the length of the PEO chains, both microgels exhibit zeta potentials with very weak pH dependence (approximately ±5 mV, which corresponds to very low surface charge). This result is not particularly surprising, since the PEO chains have nonionic character and the PMPC chains are zwitterionic in nature; hence, neither component contributes any net surface charge. Similar observations have been made for PMPC-stabilized polystyrene latexes prepared by conventional radical polymerization.[28]

Figure 12 shows the effect of added NaCl on the mean DLS diameter and polydispersity for a series of cross-linked PEO-*b*-PMPC swollen microgels dispersed in water (entries 7 and 9 in Table 2). Irrespective of the degree of cross-linking targeted using EGDMA, both parameters remain essentially unchanged irrespective of the concentration of added salt. This is due to the well-known "anti-polyelectrolyte effect",[54,55] which characterizes the aqueous solution properties of polyzwitterions such as PMPC. Conventional polyelectrolytes are highly swollen at low salt concentration but collapse at higher salt concentration due to charge screening, which reduces electrostatic repulsion between the anionic or cationic chains.[56,57] In contrast, polyzwitterions such as PMPC remain highly solvated in the presence of high concentrations of added salt and their chain dimensions remain more or less constant.

Conclusions

Novel sterically stabilized PMPC nanolatexes were prepared via dispersion polymerization using a PEO-based ATRP macroinitiator with either EGDMA or BPDMA (or no cross-linker) in a 9:1 IPA/water mixture at 40 °C. ^{1}H NMR studies confirmed that the PMPC chains formed the nanolatex cores under these conditions due to a known co-nonsolvency phenomenon, while the PEO chains act as the steric stabilizer. The mean diameters of cross-linked nanolatexes were similar to the corresponding linear nanolatexes and ranged from 50 to 512 nm. On dialysis against water, the cross-linked particles became highly swollen microgels (with mean diameters ranging from 81 to 830 nm) but retained their narrow size distributions. However, relatively high levels of cross-linker (e.g., 10 mol % EGDMA) were required to prevent dissolution of non-cross-linked diblock copolymer chains. The dimensions of these nanolatexes are affected by the precise polymerization formulation, particularly the monomer concentration and the target degree of polymerization of the core-forming PMPC chains, as judged by DLS, SEM, and TEM. XPS studies confirmed the presence of the PEO chains at the particle surface and allowed their surface coverage to be estimated. Aqueous electrophoresis studies indicated that zeta potentials varies only weakly with solution pH over a wide range of pH, as expected given the nonionic and zwitterionic nature of the PEO and PMPC chains, respectively. Dialysis of these novel particles in their swollen microgel form removed essentially all of the toxic ATRP catalyst. DLS studies confirmed that the purified particles are highly resistant to salt-induced flocculation. These novel particles can be conveniently labeled by simply incorporating a fluorescent comonomer, which suggests that they may have potential biomedical applications, e.g., in live cell imaging. This possibility will be explored in future work.

Acknowledgment. S.S. thanks JSPS Postdoctoral Fellowships for a Research Abroad grant, and Biocompatibles is thanked for supplying the MPC monomer and for permission to publish this work.

References and Notes

(1) Kawaguchi, H. *Prog. Polym. Sci.* **2000**, *25*, 1171–1210.
(2) Sukhorukov, G.; Fery, A.; Möhwald, H. *Prog. Polym. Sci.* **2005**, *30*, 885–897.
(3) Chern, C. S. *Prog. Polym. Sci.* **2006**, *31*, 443–486.
(4) Motornov, M.; Roiter, Y.; Tokarev, I.; Minko, S. *Prog. Polym. Sci.* **2010**, *35*, 174–211.
(5) Boury, F.; Marchais, H.; Benoit, J. P.; Proust, J. E. *Biomaterials* **1997**, *18*, 125–136.
(6) Bourgeat-Lami, E.; Tissot, I.; Lefebvre, F. *Macromolecules* **2002**, *35*, 6185–6191.
(7) Ahmad, H.; Tauer, K. *Macromolecules* **2003**, *36*, 648–653.
(8) Mahdavian, A. R.; Abdollahi, M. *React. Funct. Polym.* **2006**, *66*, 247–254.
(9) Mohanty, P. S.; Dietsch, H.; Rubatat, L.; Stradner, A.; Matsumoto, K.; Matsuoka, H.; Schurtenberger, P. *Langmuir* **2009**, *25*, 1940–1948.
(10) Duan, L.; Chen, M.; Zhou, S.; Wu, L. *Langmuir* **2009**, *25*, 3467–3472.
(11) Collins, E. A. In *Emulsion Polymerization and Emulsion Polymers*; Lovell, P. A., El-Aasser, M. S., Eds.; John Wiley and Sons, Ltd.: Chichester, 1997; pp 385−436.
(12) (a) Li, W.; Min, K.; Matyjaszewski, K.; Stoffelbach, F.; Charleux, B. *Macromolecules* **2008**, *41*, 6387–6392. (b) Min, K.; Gao, H.; Matyjaszewski, K. *J. Am. Chem. Soc.* **2006**, *128*, 10521–10526. (c) Li, M.; Min, K.; Matyjaszewski, K. *Macromolecules* **2004**, *37*, 2106–2112. (d) Li, M.; Matyjaszewski, K. *Macromolecules* **2003**, *36*, 6028–6035.
(13) (a) Kagawa, Y.; Kawasaki, M.; Zetterlund, P. B.; Minami, H.; Okubo, M. *Macromol. Rapid Commun.* **2007**, *28*, 2354–2360.

(b) Kagawa, Y.; Zetterlund, P. B.; Minami, H.; Okubo, M. *Macromolecules* **2007**, *40*, 3062–3069. (c) Okubo, M.; Minami, H.; Zhou, J. *Colloid Polym. Sci.* **2004**, *282*, 747–752.
(14) Napper, D. H. *Polymeric Stabilization of Colloid Dispersions*; Academic Press: London, 1983.
(15) Kawaguchi, S.; Ito, K. *Adv. Polym. Sci.* **2005**, *175*, 299–328.
(16) Barrett, K. E. J. *Dispersion Polymerization in Organic Media*, 1st ed.; John Wiley and Sons: London, 1975.
(17) Ali, A. M. I.; Pareek, P.; Sewell, L.; Schmid, A.; Fujii, S.; Armes, S. P.; Shirley, I. M. *Soft Matter* **2007**, *3*, 1003–1013.
(18) Horák, D.; Švec, F.; Fréchet, J. M. J. *J. Polym. Sci., Part A: Polym. Chem.* **1995**, *33*, 2961–2968.
(19) Hawker, C. J.; Bosman, A. W.; Harth, E. *Chem. Rev.* **2001**, *101*, 3661–3688.
(20) (a) Kamigaito, M.; Ando, T.; Sawamoto, M. *Chem. Rev.* **2001**, *101*, 3689–3745. (b) Kato, M.; Kamigaito, M.; Sawamoto, M.; Higashimura, T. *Macromolecules* **1995**, *28*, 1721–1723.
(21) (a) Matyjaszewski, K.; Xia, J. *Chem. Rev.* **2001**, *101*, 2921–2990. (b) Wang, J.-S.; Matyjaszewski, K. *J. Am. Chem. Soc.* **1995**, *117*, 5614–5615. (c) Wang, J.-S.; Matyjaszewski, K. *Macromolecules* **1995**, *28*, 7901–7910.
(22) (a) Chiefari, J.; Chong, Y. K.; Ercole, F.; Krstina, J.; Jeffery, J.; Le, T. P. T.; Mayadunne, R. T. A.; Meijs, G. F.; Moad, C. L.; Moad, G.; Rizzardo, E.; Thang, S. H. *Macromolecules* **1998**, *31*, 5559–5562. (b) Moad, G.; Rizzardo, E.; Thang, S. H. *Polymer* **2008**, *49*, 1079–1131.
(23) Zetterlund, P. B.; Kagawa, Y.; Okubo, M. *Chem. Rev.* **2008**, *108*, 3747–3794.
(24) Gabaston, L. I.; Jackson, R. A.; Armes, S. P. *Macromolecules* **1998**, *31*, 2883–2888.
(25) Qiu, J.; Charleux, B.; Matyjaszewski, K. *Prog. Polym. Sci.* **2001**, *26*, 2083–2134.
(26) Wan, W.-M.; Pan, C.-Y. *Macromolecules* **2007**, *40*, 8897–8905.
(27) (a) Lobb, E. J.; Ma, I.; Billingham, N. C.; Armes, S. P. *J. Am. Chem. Soc.* **2001**, *123*, 7913–7914. (b) Ma, I. Y.; Lobb, E. J.; Billingham, N. C.; Armes, S. P.; Lewis, A. L.; Lloyd, A. W.; Salvage, J. *Macromolecules* **2002**, *35*, 9306–9314. (c) Li, C.; Madsen, J.; Armes, S. P.; Lewis, A. L. *Angew. Chem., Int. Ed.* **2006**, *45*, 3510–3513.
(28) Thompson, K. L.; Bannister, I.; Armes, S. P.; Lewis, A. L. *Langmuir* **2010**, *26*, 4693–4702.
(29) Sugihara, S.; Armes, S. P.; Lewis, A. L. *Angew. Chem., Int. Ed.* **2010**, *49*, 3500–3503.
(30) Edmondson, S.; Nguyen, N. T.; Lewis, A. L.; Armes, S. P. *Langmuir* **2010**, *26*, 7216−7226.
(31) Lewis, A. L. *Colloids Surf., B* **2000**, *18*, 261–275.
(32) Iwasaki, Y.; Ishihara, K. *Anal. Bioanal. Chem.* **2005**, *381*, 534–546.
(33) Massignani, M.; LoPresti, C.; Blanazs, A.; Madsen, J.; Armes, S. P.; Lewis, A. L.; Battaglia, G. *Small* **2009**, *5*, 2424–2432.
(34) Moro, T.; Takatori, Y.; Ishihara, K.; Konno, T.; Takigawa, Y.; Matsushita, T.; Chung, U.-I.; Nakamura, K.; Kawagushi, H. *Nature Mater.* **2004**, *3*, 829–836.
(35) Du, J.; Tang, Y.; Lewis, A. L.; Armes, S. P. *J. Am. Chem. Soc.* **2005**, *127*, 17982–17983.
(36) Lomas, H.; Canton, I.; MacNeil, S.; Du, J.; Armes, S. P.; Ryan, A. J.; Lewis, A. L.; Battaglia, G. *Adv. Mater.* **2007**, *19*, 4238–4243.
(37) Ishihara, K.; Nomura, H.; Mihara, T.; Kurita, K.; Iwasaki, Y.; Nakabayashi, N. *J. Biomed. Mater. Res.* **1998**, *39*, 323–330.
(38) Feng, W.; Nieh, M.-P.; Zhu, S.; Harroun, T. A.; Katsaras, J.; Brash, J. L. *Biointerphases* **2007**, *2*, 34–43.
(39) Sugiyama, K.; Aoki, H. *Polym. J.* **1994**, *26*, 561–569.
(40) Watanabe, J.; Ishihara, K. *Biomacromolecules* **2006**, *7*, 171–175.
(41) Park, J.; Kurosawa, S.; Watanabe, J.; Ishihara, K. *Anal. Chem.* **2004**, *76*, 2649–2655.
(42) Goto, Y.; Matsuno, R.; Konno, T.; Takai, M.; Ishihara, K. *Biomacromolecules* **2008**, *9*, 828–833.
(43) Lewis, A. L.; Hughes, P. D.; Kirkwood, L. C.; Leppard, S. W.; Redman, R. P.; Tolhurst, L. A.; Stratford, P. W. *Biomaterials* **2000**, *21*, 1847–1859.
(44) (a) Kiritoshi, Y.; Ishihara, K. *J. Biomater. Sci., Polym. Ed.* **2002**, *13*, 213–224. (b) Matsuda, Y.; Kobayashi, M.; Annaka, M.; Ishihara, K.; Takahara, A. *Polym. J.* **2008**, *40*, 479–483.
(45) Ahmad, H.; Dupin, D.; Armes, S. P.; Lewis, A. L. *Langmuir* **2009**, *25*, 11442–11449.
(46) Riley, T.; Govender, T.; Stolnik, S.; Xiong, C, D.; Garnett, M. C.; Illum, L.; Davis, S. S. *Colloids Surf., B* **1999**, *16*, 147–159.
(47) Liu, S.; Weaver, J. V. M.; Tang, Y.; Billingham, N. C.; Armes., S. P.; Tribe, K. *Macromolecules* **2002**, *35*, 6121–6131.
(48) Ma, Y.; Tang, Y.; Billingham, N. C.; Armes, S. P.; Lewis, A. L.; Lloyd, A. W.; Salvage, J. P. *Macromolecules* **2003**, *36*, 3475–3484.
(49) Flick, E. W. *Industrial Solvents Handbook*, 5th ed.; Noyes Data Corporation: Westwood, NJ, 1998; Chapter 6.
(50) Bütün, V.; Armes, S. P.; Billingham, N. C. *Polymer* **2001**, *42*, 5993–6008.
(51) Rosselgong, J.; Armes, S. P.; Barton, W. R. S.; Price, D. *Macromolecules* **2010**, *43*, 2145–2156.
(52) Minami, H.; Yoshida, K.; Okubo, M. *Macromol. Rapid Commun.* **2008**, *29*, 567–572.
(53) Yuting, L.; Armes, S. P. *Angew. Chem., Int. Ed.* **2010**, *49*, 4042–4046.
(54) Matsuda, Y.; Kobayashi, M.; Annaka, M.; Ishihara, K.; Takahara, A. *Chem. Lett.* **2006**, *35*, 1310–1311.
(55) Mahon, J.; Zhu, S. *Colloid Polym. Sci.* **2008**, *286*, 1443–1454.
(56) Eliassaf, J.; Silberberg, A. *J. Polym. Sci., Polym. Chem. Ed.* **2003**, *41*, 31–35.
(57) Guo, L.; Tam, K. C.; Jenkins, R. D. *Macromol. Chem. Phys.* **1998**, *199*, 1175–1184.